Journal of Archaeological Science 49 (2014) 472–487

Contents lists available at ScienceDirect

Journal of Archaeological Science

journal homepage: http://www.elsevier.com/locate/jas

The role of raw material differences in stone tool shape variation: an experimental assessment

Metin I. Eren [a, b, *], Christopher I. Roos [c], Brett A. Story [d], Noreen von Cramon-Taubadel [e], Stephen J. Lycett [e]

[a] Department of Anthropology, University of Missouri, Columbia, MO, 65211, USA
[b] Department of Archaeology, Cleveland Museum of Natural History, Cleveland, OH 44106-1767, USA
[c] Department of Anthropology, Southern Methodist University, Dallas, TX 75275, USA
[d] Department of Civil and Environmental Engineering, Southern Methodist University, Dallas, TX 75275, USA
[e] Department of Anthropology, University at Buffalo SUNY, 380 MFAC-Ellicott Complex, Buffalo, NY 14261-0005, USA

ARTICLE INFO

Article history:
Received 27 March 2014
Received in revised form
29 May 2014
Accepted 30 May 2014
Available online 12 June 2014

Keywords:
Raw material
Handaxes
Experimental archaeology
Acheulean
Experiment

ABSTRACT

Lithic raw material differences are widely assumed to be a major determining factor of differences in stone tool morphology seen across archaeological sites, but the security of this assumption remains largely untested. Two different sets of raw material properties are thought to influence artifact form. The first set is internal, and related to mechanical flaking properties. The second set is external, namely the form (size, shape, presence of cortex) of the initial nodule or blank from which flakes are struck. We conducted a replication experiment designed to determine whether handaxe morphology was influenced by raw materials of demonstrably different internal and external properties: flint, basalt, and obsidian. The knapper was instructed to copy a "target" model handaxe, produced by a different knapper, 35 times in each toolstone type ($n = 105$ handaxes). On each experimental handaxe, 29 size-adjusted (scale-free) morphometric variables were recorded to capture the overall shape of each handaxe in order to compare them statistically to the model. Both Principal Components Analysis (PCA) and a Multivariate Analysis of Variance (MANOVA) were used to determine if raw material properties were a primary determinate of patterns of overall shape differences across the toolstone groups. The PCA results demonstrated that variation in all three toolstones was distributed evenly around the model target form. The MANOVA of all 29 size-adjusted variables, using two different tests, showed no statistically significant differences in overall shape patterns between the three groups of raw material. In sum, our results show that assuming the primacy of raw material differences as the predominant explanatory factor in stone tool morphology, or variation between assemblages, is unwarranted.

1. Introduction

Understanding the role that stone raw materials played in lithic artifact form and assemblage variability is an issue fundamental to archaeological research in all times and places in which flaked stone technology was utilized. Indeed, raw material "quality" has long been cited as a potentially important factor influencing lithic artifact morphology (Abbott, 1911; Goodman, 1944). Despite the fact that "quality" is often a subjective, poorly defined characteristic of knappable stone, for which there is no consensus (Brantingham et al., 2000; Braun et al., 2009; Browne and Wilson, 2011), several lithic analysts have emphasized the role that stone raw material "quality" plays in artifact form. For instance, Andrefsky (1994:23) suggested that the "quality" of lithic raw materials is one of the two most important factors in the organization of stone technology (the other being lithic "abundance"), and that "the quality … of lithic raw materials played a direct role in prehistoric tool makers decisions to produce various types of stone tools." Twenty years on, Manninen and Knutsson (2014:95) underscore this notion, stating that "when lithic technological organization is viewed as an intersection of many varying dimensions, the properties and availability of raw materials can be considered the most important determinants in how these dimensions intersect within any organizational context."

The motivation for these inferences perhaps stems from the inevitable co-variation between particular stone raw materials and

* Corresponding author. Department of Anthropology, University of Missouri, Columbia, MO 65211, USA.
E-mail address: metin.i.eren@gmail.com (M.I. Eren).

http://dx.doi.org/10.1016/j.jas.2014.05.034
0305-4403/

particular tool forms (or lithic reduction strategies) at archaeological localities. As Brantingham et al. (2000:257) explain:

> The assumption is that the ability to execute formal technological designs is severely limited by the quality of the raw material. Toolkits based on high quality raw materials are thought to be easier to design because fracture is easier to control (Goodyear, 1989:3; Luedtke, 1992). In contrast, toolkits based on poor quality raw material are more difficult to design because fracture is unpredictable and results in severe, irreparable errors during reduction. Even where low raw material abundance would encourage formal technological design, raw material quality is thought to be the overriding factor constraining lithic technological organization.

While the archaeological co-variation between particular stone types and artifact morphologies certainly suggests that––in certain times and places––raw material differences were an influence on artifact morphology, it still remains to be determined whether raw material *automatically* influences stone tool form regardless of other input variables. The manner in which raw material interacts with other input variables can potentially be conceived of in two different ways. One of these is explicitly identified by Costa (2010:36) as "artificial forces" and by de la Torre (2011:788) as "technical incompetence." This suggests that raw material influenced stone artifact morphology because hominins did not possess the knowledge, manual dexterity, skills, or incentive to tackle "challenging" raw materials. This hypothesis does not suggest that raw material plays *no* role in artifact form, but instead that there is nothing *inherent* to specific "knappable" rock types that automatically or necessarily influences artifact morphology in specific ways, and thus the source of artifact form ultimately lies with hominins themselves.

The second hypothesis identified by Costa (2010:36) and de la Torre (2011:788), respectively, is "natural forces" or "raw material constraints" hypothesis (see also Sharon, 2008). This hypothesis posits that raw material "determines" artifact morphology because it is physically impossible to create similar tool forms via flintknapping on substantially different raw materials. This hypothesis is different from the first because it suggests that rather than the interaction of behavioral and cultural factors with physical/geological ones, the dominant source of artifact morphology lies exclusively within the raw material itself; i.e. there exist natural raw material constraints that "dictate" artifact morphology.

It is plausible that the stone raw materials utilized by hominins may have dictated which artifact forms they could ultimately produce. When distinct isotropic rocks––i.e. those generally free of major cleavage planes or other inclusions that inhibit the free passage of energy––are compared directly, they often exhibit differing "internal" and/or "external" properties. Stone raw material "internal properties" consist of attributes relevant to the mechanical process of crack initiation and propagation, i.e. elasticity, brittleness, hardness, homogeneity, granularity, and isotropy (Goodman, 1944; Callahan, 1979; Whittaker, 1994; Andrefsky, 1998). "External properties" refer to the form (size, shape, surface regularity, cortex presence, etc.) of the initial nodule, block, or blank from which flakes are struck (Ashton and McNabb, 1994; Eren et al., 2011a; Jennings et al., 2010; Smallwood, 2010). However, despite these factors, several recent archaeological studies have questioned the automatic primacy of such constraints in determining artifact form (e.g., Brantingham et al., 2000; Sharon, 2008; Archer and Braun, 2010; Costa, 2010; Clarkson, 2010; Smallwood, 2012; Buchanan et al., 2014; Lycett and von Cramon-Taubadel, 2014). As intimated above, there remains a distinct risk that raw material factors are considered a dominant, if not sole, determinant of stone artifact morphology purely as a result of the coincidence between different raw materials and different artifact morphologies at different archaeological sites.

We are skeptical of the extent to which further studies of the archaeological record alone can contribute to these debates. For stone "constraints" to be tested, knowledge of both knapper intention and skill must be controlled (i.e. held constant across materials), and in prehistoric contexts these attributes remain unknown to the archaeologist. For instance, if a lithic analyst discovers a pattern in which thinner bifaces (on average) are made on "high quality" stone type A and thicker bifaces are made on "low quality" stone type B, it would be impossible to resolve whether (i) raw material constrained artifact form, (ii) the knapper(s) did not have the skill to make type B handaxes as thin as the type A ones, or (iii) there was some other behavioral or cultural reason that caused the knapper(s) to manufacture type B handaxes thicker than type A ones. For this reason, several lithic analysts have called for experimental tests to "document the impact of the properties of raw materials on the way in which particular tool types were produced" (Holdoway and Stern, 2004:55; see also Bar-Yosef et al., 2012:12). Indeed, over 70 years ago, Goodman (1944:431) advocated that experiments be conducted that examine "the degree to which the nature of the [stone] material in a person's hand may have guided or limited the work done upon that material by the artisan."

In response to these calls, Eren et al. (2011a) conducted a 20-month long lithic replication experiment to determine whether, with continuous practice, a knapper's advancing skill in preferential Levallois flake production would be statistically identifiable if the high quality toolstone used was switched to a less tractable chert. Specific quantitative knapping goals were measured and assessed statistically, and overall the results showed that factors associated with knapping skill, rather than raw material quality, were the main causes of success or failure in achieving the set knapping goals. Although these results were inconsistent with the raw material constraints hypothesis, Eren et al. (2011a:2738) recognized the necessity of further experimental assessments. The two toolstones used in the Eren et al. (2011a:2738) experiment contrasted in both their internal and external properties, but both materials could be classified as "chert" in its broadest definition (Luedtke, 1992) and thus differed less prominently in their internal flaking properties than in their external properties. Furthermore, the knapping goals in that experiment involved individual morphological or economic attributes rather than holisitic assessments of gross morphology, leaving open to question the relationship between stone raw material differences and overall stone tool form.

Here, directly expanding upon the experiments of Eren et al. (2011a), we report a replication experiment that tested directly whether different stone raw material categories necessarily constrain artifact shape. The experiment examined three distinct stone raw materials––flint, basalt, and obsidian—which possessed different external and internal properties, and tested whether any of these materials prevented a knapper from successfully copying the shape of a replica handaxe model similar to those produced during the Late Acheulean. We chose this model for the experiment––acknowledging that future work should examine other tool types and reduction strategies––for two reasons. First, this particular tool type would provide a challenge to the knapper within the context of Lower Paleolithic technology (see e.g., Callahan, 1979; Edwards, 2001; Schick, 1994; Winton, 2005). Second, the influence of raw material differences on handaxe form has been debated extensively (e.g., Isaac, 1977; Jones, 1979; Wynn and Tierson, 1990; Roe, 1994; Schick, 1994; Clark, 2001; McPherron, 2006; Sharon, 2008; Archer and Braun, 2010; Costa, 2010; Lycett and Bae, 2010; Gowlett, 2011; Bar-Yosef et al., 2012; Diez-Martin and Eren, 2012), and thus the present experiment will contribute

directly to these widespread debates from a somewhat different angle.

If, as predicted by the raw material constraints hypothesis, stone raw material differences determine handaxe form, then (1) there should be significant inter-group shape differences between two or more raw material groups; and (2), one or more raw material groups should deviate significantly in shape from the model. Accordingly, we tested these predictions via a series of statistical analyses and a measurement protocol designed to capture the three-dimensional shape of each handaxe, consisting of 29 size-adjusted morphometric variables.

2. Materials and methods

2.1. Knapping the handaxe dataset

An experienced knapper (MIE) was instructed to copy a model handaxe (Fig. 1) 35 times in three raw materials (flint, basalt, and obsidian) for a total sample of 105 handaxes (Fig. 2). To ensure independence between the experimental knapper and the model he was copying, the model was produced by another experienced knapper (SJL) on a flint raw material different than that used in the experimental dataset. The model flint was procured from a beach in Kent (UK), while the flint used for the experimental dataset (described below) was procured from an inland quarry approximately 115 km north of this in Suffolk. To guarantee that the experimental knapper was sufficiently challenged, and that any potential raw material constraints were rigorously investigated within the parameters of Lower Paleolithic handaxe technology, the target model deliberately exhibited high symmetry in both plan- and profile-view, possessed a high width-to-thickness ratio (W:T = 3.33), and displayed relatively flat faces with no irregularities.

To ensure that learning over time did not confound results, materials were knapped rotationally (flint, basalt, and obsidian). In order to minimize fatigue factors, only three handaxes were produced per day, with breaks between each nodule. Knapping thus took place over a period of 35 days. The same set of knapping tools was used throughout, which consisted of three moose antlers, a sandstone hammerstone, and three granite hammerstones (Table 1).

Fig. 1. The model handaxe produced by SJL on a flint raw material different than that used in the experimental dataset. The model flint was procured from a beach in Kent (UK).

2.2. Raw materials

The flint used for the experimental dataset was procured from an inland quarry near Bury St. Edmunds, in the county of Suffolk, UK (Fig. 3a). It was the only raw material that exhibited cortex, and many of the flint nodules possessed outer surfaces that were over 80% cortical. We also note that of the three raw materials, it possessed the most natural flaws, with eight of the thirty-five nodules possessing major cleavages, "concrete" inclusions, or crystal pockets. The basalt was procured from the Partridge Creek area of Yavapai county, Arizona, USA (Fig. 3b, left). Only three of the thirty-five nodules possessed a natural cleavage. The obsidian was procured from the Glass Buttes mountain range in Lake County, Oregon, USA (Fig. 3b, right), it was a flaw-free stone. These three particular raw materials were selected because the experimental knapper was not familiar with them, and thus "previous experience" was minimized as a potential confounding factor of inter-group comparisons. That said, the use of an experienced knapper was vital to the experiment (MIE has 13 years of knapping experience and can replicate a range of Paleolithic technologies with a high degree of accuracy). The use of a novice or intermediate knapper for this particular experiment could potentially obscure the results in the event that handaxes from one or more raw material groups differed significantly from the model: it would be unclear whether inherent raw material "constraints" were driving the differences, or whether the novice or intermediate knapper did not possess the knowledge or skill with which to approach the raw materials.

In order to move beyond the assumption that the properties of these stone raw materials were different merely because they are different rock types, we conducted several different empirical tests and examinations to better understand how these raw materials differed with regard to several of their external and internal properties. Comparisons of external properties included the nodule size and nodule shape. Comparisons of internal properties included observations from thin-sections, scanning electron microscopy of fresh fracture surfaces, rebound hardness, and biaxial flexure.

2.2.1. External properties

2.2.1.1. Starting nodule size. The initial sizes of nodules across raw material categories were compared using the geometric mean of seven different dimensional variables taken on each nodule prior to reduction. The geometric mean is an appropriate measure of size for individual objects when using dimensional data (Jungers et al., 1995), and is preferable to mass when comparing across objects of differing material due to potential differences in density. The seven dimensional variables used were maximum nodule length (in any orientation), width at 25%, 50%, and 75% of length, and thickness at 25%, 50%, 75% of length, where the latter six measurements were all taken orthogonally to maximum length (Table 2). Fig. 4 shows the variation in computed geometric mean values across the three different raw material categories in the form of box plots.

If initial nodule sizes differ systematically across different raw material categories, we would expect statistically significant differences in the computed geometric mean values across categories. Hence, the null hypothesis is that there would be no statistical differences in the geometric mean values across the three different categories of raw material. This hypothesis was tested using a Kruskal–Wallis test, where $\alpha = 0.05$.

Fig. 2. All 105 replicated handaxes. Handaxe #1 is upper leftmost specimen, and the handaxes proceed in rows going from left to right. Handaxe #105 is lower rightmost specimen. Due to the angle at which this photograph was taken, the handaxes towards the top of the image look wider than they are in reality.

The Kruskal–Wallis test indicated highly significant differences between the different raw material types ($H = 51.80$; $p < 0.0001$). Hence, initial nodule sizes were not statistically equivalent across raw material categories. Post-hoc Mann–Whitney U tests indicated that all pairwise comparisons between raw material categories were highly significant ($p < 0.0001$), indicating that each raw material was statistically different in size from the others.

2.2.1.2. Starting nodule shape. An assessment of starting nodule shape differences across different raw material categories was undertaken. Seven variables were used: maximum nodule length (in any orientation), width at 25%, 50%, and 75% of length, and thickness at 25%, 50%, and 75% of length, where the latter six measurements were all taken orthogonally to maximum length (Table 2). To transform these dimensions into shape variables, each variable was size-adjusted using the geometric mean method (see below, Section 2.3.1).

If the initial shape of nodules differs across raw material categories, then, statistically significant differences should be found across categories. This prediction was tested using a MANOVA ($\alpha = 0.05$) of all seven size-adjusted variables, using two different test statistics (Pillai's Trace and Wilks' Lambda).

MANOVA of size-adjusted shape variables for nodules indicated highly significant differences for the shape of nodules in different categories (Pillai's Trace: $F = 4.88$, df $= 194$, $p < 0.0001$; Wilks' Lambda: $F = 4.912$, df $= 192$, $p < 0.0001$). Post-hoc analyses (Bonferroni) indicated that all raw material categories were significantly different from each other on at least one variable, while all raw material groups were significantly different from one other group on a minimum of four variables.

Table 1
The only knapping tools used for the experimental replications.

Tool	Mass (g)	Length (mm)	Width (mm)	Thickness (mm)
Moose Antler	900	270	58	50
Moose Antler	600	220	43	38
Moose Antler	600	170	49	47
Sandstone Hammerstone	1000	120	84	62
Granite Hammerstone	800	100	89	62
Granite Hammerstone	900	90	83	72
Granite Hammerstone	300	60	60	53

2.2.2. Internal properties

2.2.2.1. Microscopic observations from thin-sections and fracture surfaces. Four thin sections of each raw material category were examined for microstructure, fabric, and mineralogy in transmitted

Fig. 3. The flint used for the experimental dataset was procured from an inland quarry near Bury St. Edmunds, in the county of Suffolk, UK (a). The basalt was procured from the Partridge Creek area of Yavapai county, Arizona, USA (b, left). The obsidian was procured from the Glass Buttes mountain range in Lake County, Oregon, USA (b, right).

brightfield polarized and cross-polarized light at magnifications ranging from 7× to 200× on stereozoom and petrographic microscopes. We were primarily concerned with identifying the abundance and spatial distribution of mineral grains within the non-crystalline (obsidian and basalt) and crypto-crystalline (flint) matrices of the toolstone materials. Large, abundant, and closely spaced crystalline minerals would pose discontinuities to the propagation of force through the toolstone medium and should make knapping a more unpredictable process, whereas small, rare, and widely spaced grains should make a material easier to knap. Additionally, the ventral surface of freshly removed flakes of each raw material was examined without a coating in variable pressure scanning electron microscope (Leo-Zeiss 1450VPSE). In our SEM observations, we were particularly interested in observing the structure of cleavage plains as a means of identifying the portion of the matrix through which force actually propagated and to what extent crystalline minerals interfered with the transmission of force.

The flint material used in this study varied considerably in the degree of decalcification in correspondence with the macroscopic color of the material (Fig. 5). Black flint zones are predominantly very fine-grained microcrystalline quartz with rare (<5%) 200–500 μm sized domains of chalcedonic quartz intergrowths, often as fossil pseudomorphs or as replacement features in etched calcite domains. Sub-rounded 100–150 μm micro-sparitic calcite domains are extremely rare (<1%).

By contrast, dark gray flint zones are fossiliferous, calcareous microcrystalline quartz with common (10–15%) angular to subangular, etched micro-sparitic and micritic calcite fossil shell fragments and spherules of calcite infilled with microcrystalline quartz. These are generally fairly closely spaced with very fine sand-sized grains (up to 150 μm) typically spaced 50–100 μm apart whereas silt-sized grains (<63 μm) are typically spaced less than 25 μm apart.

Light gray zones of the flint are very heterogeneously decalcified microcrystalline quartz with rare (<5%) subangular, coarse (1000–2000 μm) sandy micritic limestone fragments and rare, angular microsparitic shell fragments that are widely spaced (>300 μm). At higher magnification, very fine (5–15 μm) micrite grains are widely dispersed (5–10% abundance, >100 μm spacing). Very coarse (1000–2000 μm), irregular zones of chalcedonic quartz are extremely rare (<1%).

Surprisingly, the "concrete" zones of the flint were the most decalcified of the flint zones. What appears to give the "concrete" zones their distinct character is the presence of uncommon (~2%) 200–700 μm rounded voids and abundant, dark purple (PPL) isotropic (XPL) punctuations throughout. In PPL, the "concrete" zone has a dirty, pale brown speckled color to it and it is extremely dark in XPL (note that the gain is enhanced in Fig. 5 for the "concrete" specimen in XPL to enhance the visibility of the microstructure). Its microstructure, however, is predominantly decalcified microcrystalline quartz with variable sized

Table 2
Summary statistics of recorded morphometric data from the flint, basalt, and obsidian nodules. Mass was measured in kilograms (kg), all other measurements were measured in millimeters (mm). SD = standard deviation, Q1 = quartile 1, Q3 = quartile 3.

Flint ($n = 35$)	Mass	Max. Length	Width 25%	Width 50%	Width 75%	Thickness 25%	Thickness 50%	Thickness 75%
Mean	4.4	242.3	136.7	167.5	138.2	71.2	74.7	68.1
SD	1.5	28.7	30.3	26.1	27.2	16.3	15.8	15.6
Minimum	2.0	190.0	80.0	124.0	80.0	43.0	49.0	40.0
Q1	3.6	225.0	113.5	145.0	120.0	58.5	65.0	57.0
Median	4.0	240.0	135.0	168.0	131.0	71.0	74.0	68.0
Q3	5.0	255.0	162.0	183.0	165.0	82.0	83.0	75.0
Maximum	9.0	340.0	200.0	235.0	188.0	103.0	110.0	112.0
Basalt ($n = 35$)	Mass	Max. Length	Width 25%	Width 50%	Width 75%	Thickness 25%	Thickness 50%	Thickness 75%
Mean	6.3	291.9	153.9	172.8	140.9	77.2	80.9	76.1
SD	1.5	35.9	29.1	25.3	28.7	20.5	18.4	16.1
Minimum	3.1	240.0	107.0	126.0	99.0	48.0	52.0	45.0
Q1	5.3	270.0	136.0	154.0	124.0	61.5	68.5	66.0
Median	6.0	280.0	145.0	166.0	138.0	73.0	77.0	78.0
Q3	7.3	305.0	172.5	195.5	152.0	94.0	86.5	85.5
Maximum	10.8	390.0	219.0	227.0	229.0	127.0	140.0	123.0
Obsidian ($n = 35$)	Mass	Max. Length	Width 25%	Width 50%	Width 75%	Thickness 25%	Thickness 50%	Thickness 75%
Mean	7.2	300.3	147.3	181.2	156.9	98.6	107.9	99.7
SD	0.8	30.0	32.0	29.7	36.3	26.8	18.2	22.0
Minimum	5.2	240.0	61.0	124.0	99.0	43.0	70.0	60.0
Q1	6.7	280.0	134.0	168.0	133.5	85.5	94.5	86.5
Median	7.3	300.0	151.0	181.0	150.0	99.0	106.0	100.0
Q3	7.6	315.0	165.5	193.0	177.5	116.5	118.5	115.5
Maximum	9.0	370.0	227.0	263.0	234.0	154.0	145.0	149.0

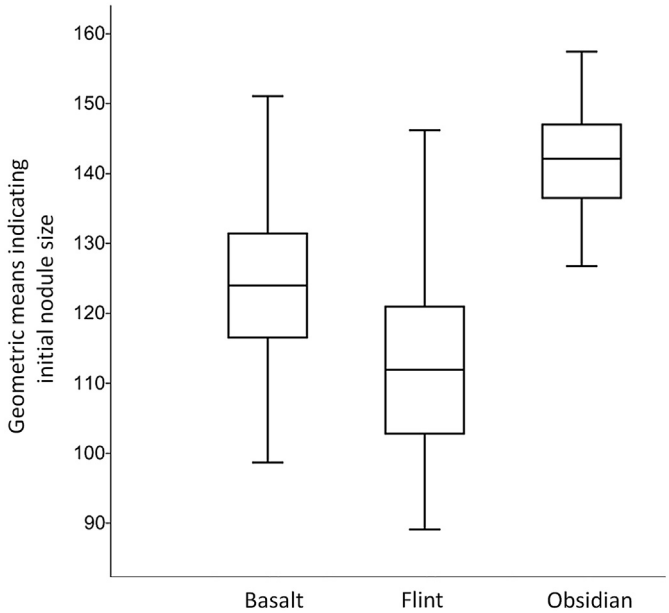

Fig. 4. Box plots of geometric mean values indicating raw size variation of initial nodules across different raw materials (box ranges indicate 25–75% quartiles with median values shown as bar within).

microcrystalline domains. Rare quartz pseudograins up to 35 μm almost give this zone the character of a fine-grained quartzite.

Fig. 6 illustrates the differences between the flint (black zone), basalt, and obsidian materials at 20×, 100×, and 200× magnification. The basalt is a fine-grained tholeiitic variety made up of mostly of ~65 μm long laths of plagioclase (~50%) and a pale brown (ppl) isotropic, glassy groundmass (~30%). Phenocrysts of quartz (extremely rare) and pyroxene (up to 200–500 μm in size) make up the remaining 20%. Phenocrysts typically occur in clusters of up to 12 grains with typical spacing between clusters of roughly 500–1100 μm. The obsidian is petrographically simple. It varies from 99 to 100% pale gray, isotropic glassy groundmass with extremely rare (0–1%) microphenocryst laths of plagioclase.

SEM observations (Fig. 7) of the flint flake indicated that the fracture preferentially occurred along crystal faces of the microcrystalline quartz groundmass with microtopgraphic irregularities created by non-quartz domains. In the basalt, fracture appears to have preferentially occurred within the glassy groundmass, occasionally interrupted by plagioclase laths, whereas in the obsidian, the fracture surface is nearly perfectly smooth as the fracture propagated through the glassy groundmass.

2.2.2.2. Fracture predictability (rebound hardness). Following Braun et al. (2009) we measured stone rebound hardness as a proxy for "fracture predictability," an attribute directly relevant to stone tool production. Rocks that fracture predictably often possess three traits (Crabtree, 1967; Domanski et al., 1994; Luedtke, 1992): (1) little or no crystalline macrostructure; (2) few impurities that could potentially interfere with fracture propagation; and (3) an overall small average crystal size. In this study, we quantitatively estimated this feature using the rebound hardness test. Rebound hardness values increase as these three raw material traits intensify in degree, while a lower magnitude of any or all of these traits results in lower rebound hardness values. Rebound hardness values were measured with a Schmidt hammer (Proceq Silver Schmidt Concrete Test Hammer PC, N-Type), which produces consistent, quantitative results comparable across rock types, and can be quickly and easily applied to large sample sizes which are then amenable to inferential statistics (Braun et al., 2009: 1607–1608).

We took 30 rebound hardness measurements from four nodule surface types: cortical flint, non-cortical flint, basalt, and obsidian. A Kruskal–Wallis test returned a highly significant values for these measurements across surface types ($H = 17.69$, $p = 0.0005$). Mann–Whitney pairwise comparisons of rebound hardness (Table 3, Fig. 8) indicated significant differences between these four surface types, but also some interesting similarities. Basalt was significantly different in rebound hardness from obsidian and non-cortical flint, but was similar to that of cortical flint. Obsidian was significantly different from basalt and cortical flint, but was similar to that of non-cortical flint. Thus, while the raw materials are indeed mostly different in terms of rebound hardness, we unexpectedly found that our experimental flint nodules possessed the qualities of both basalt and obsidian. The outside flint cortex was more like basalt, while the inner non-cortical flint was more like obsidian.

2.2.2.3. Biaxial flexure. A destructive biaxial flexure test is one method of mechanical evaluation and classification for raw materials. Archaeologically, biaxial flexure has primarily been implemented in mechanical evaluation of ceramic sherds (Neupert, 1994; Beck, 2002). However, biaxial flexure is an appropriate test method for all planar specimens (plates or shells) with irregular geometry. Tensile tests and uniaxial bending tests are carried out on uniform test specimens so that load application and support conditions do not cause undesirable effects. For example, irregular geometry can result in a loss of stability in a traditional tensile or uniaxial bending test. Additionally, a specimen may be subject to unintended forces and moments caused by eccentricity in support conditions and loading. The support conditions necessary for biaxial flexure reduce these deleterious effects by providing planar, rather than linear, boundary conditions.

A "ball-on-three-ball" biaxial flexure load apparatus was fabricated to support specimens and apply a concentrated load via the INSTRON 5582 load frame shown in Fig. 9a. Fig. 9b illustrates the apparatus in detail. Each rock plate specimen is placed atop three ball bearing supports on the bottom portion of the load apparatus; this configuration provides three points of contact and three corresponding vertical reactions necessary for vertical equilibrium of the specimen regardless of geometry (Ritter et al., 1980). The load is applied to the specimen through the single ball bearing on the top portion of the apparatus. The support bearings are located 25.4 mm equidistant from the center of the specimen. The concentrated load affects the central portion of the specimen bounded by the 25.4 mm radius. While specimens larger than this area experience some overhang, the effects of such an overhang on specimens of this size, geometry and loading are minimal (Neupert, 1994). This setup reduces inconsistencies of the loading and load distribution in each specimen. A safety barrier was placed around the loading apparatus and specimen during testing as seen in Fig. 10. This prevented the scattering of shattered fragments of each specimen at fracture.

The INSTRON 5582 load frame has a capacity of 100 kN. A load cell recorded the force applied to the specimen throughout the experiment. An extensometer was fixed to the apparatus to estimate the displacement of the rock plate under load. The experiments were conducted in displacement control with a load rate of 1 mm/min.

Destructive biaxial flexure tests were performed on plate specimens of varying thicknesses for flint, basalt, and obsidian materials. The characterizing quantity of interest in these tests was the peak force applied to the specimen immediately prior to fracture. The peak force that a specimen can withstand is a function of the applied load, material, and specimen geometry. In these experiments, the conditions of load application and support geometry were held constant. The material properties and thicknesses were varied.

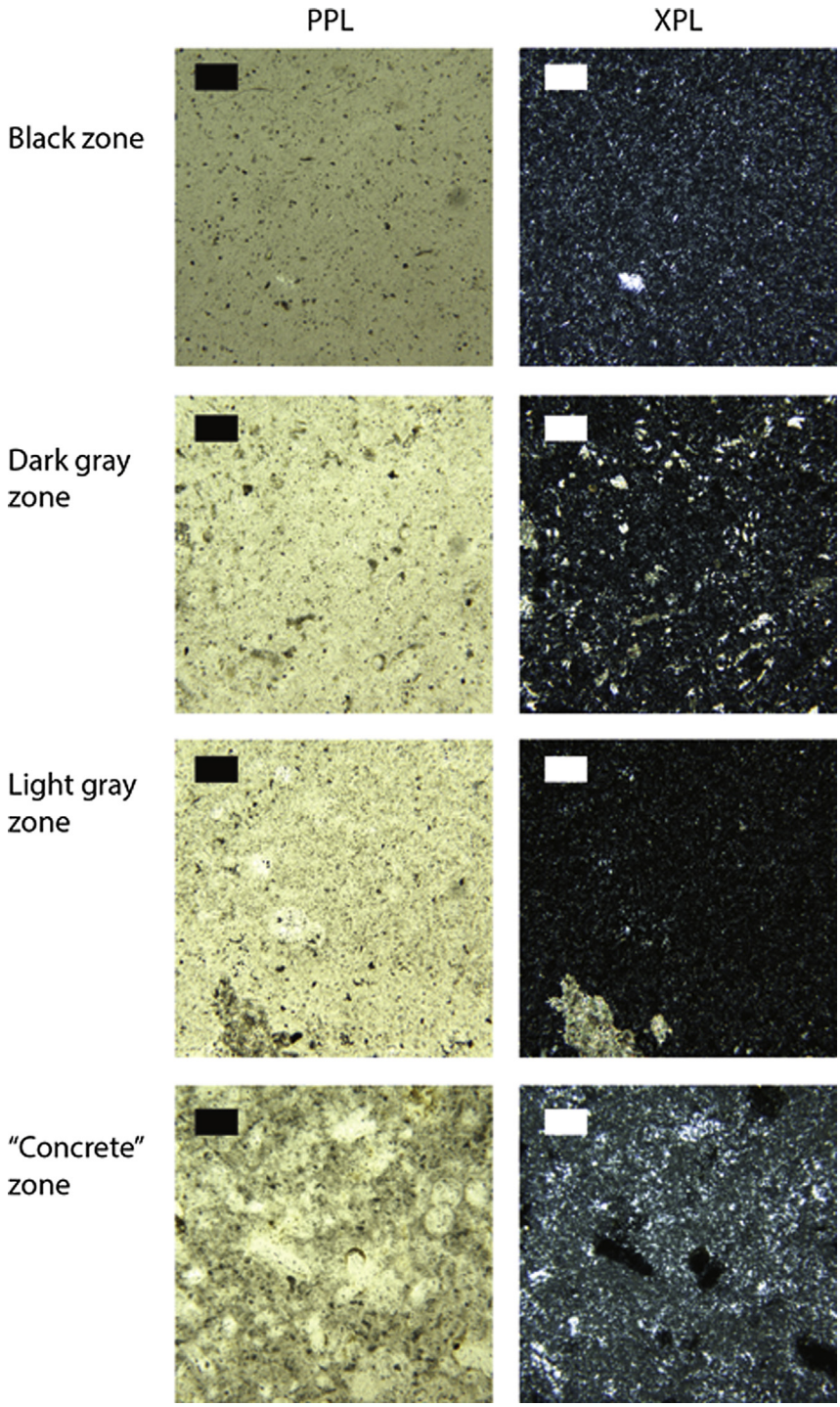

Fig. 5. Thin-sections of flint which varied considerably in the degree of decalcification in correspondence with the macroscopic color of the material. See main text for descriptions. (For interpretation of the references to color in this figure legend, the reader is referred to the web version of this article.)

The protocol for measuring the peak load force and specimen thickness was applied as follows:

(i) Place specimen on three support bearings and preload the specimen (to approximately 20 N) so that contact is ensured at the onset of testing.
(ii) Close safety barrier door and record initial preload.
(iii) Load the specimen in displacement control at 1 mm/min until fracture (indicated by instantaneous decrease in load).
(iv) Collect broken pieces and reconstruct the original specimen.
(v) Use digital calipers to measure the thickness of each piece at the point of fracture. Thickness measurement was recorded orthogonally to the long axis.
(vi) Average these thickness measurements to determine the specimen thickness.

This protocol was performed for 15 samples of each material (45 total specimens).

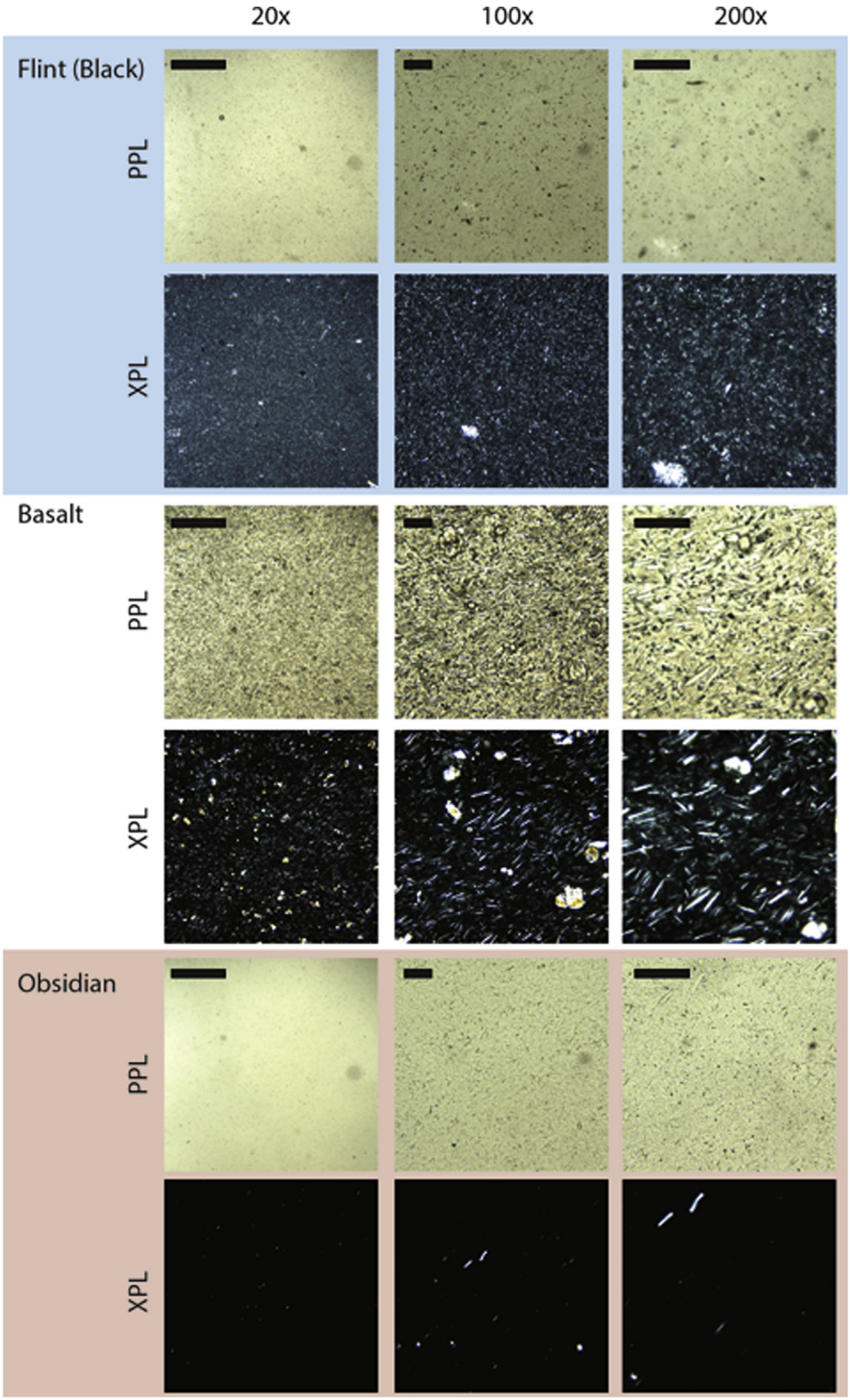

Fig. 6. Thin-section illustrates the differences between the flint (black zone), basalt, and obsidian materials at 20×, 100×, and 200× magnification. See main text for descriptions.

2.2.2.4. Biaxial flexure data analysis. Fig. 10 displays a load time history of a 9.03 mm thick Flint specimen. The peak load for this specimen was 970.74 N which occurs just after 20 s and just before fracture of the specimen. Flat regions in the time history represent instances in the test of slight shifting or sliding of the specimen. Regions of linear increase represent loading of the specimen at a constant load rate. MATLAB was used to extract peak load values for each specimen. Plots of peak load vs. specimen thickness for flint,

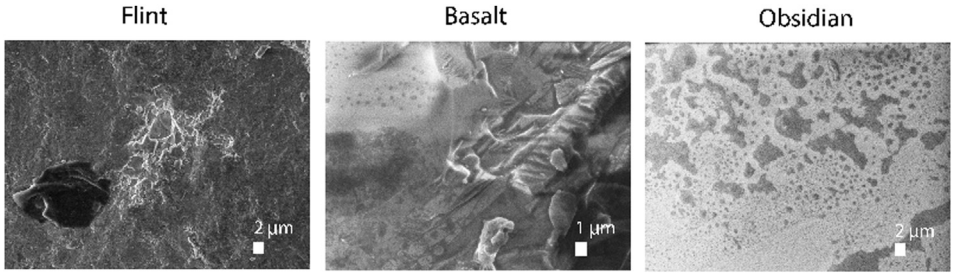

Fig. 7. SEM images of the flint, basalt, and obsidian. See main text for descriptions.

basalt, and obsidian are shown in Fig. 11. Table 4 contains linear regression equations and R^2 values for each material. The relationships between the peak load and thickness for each material may all be approximated by linear relationships, but the three relationships are distinct.

Eq. 1–3 in Table 3 distinguish the behavior of each of the three types of raw materials examined. Peak loads for each material were 13.60 kN ($t = 14.41$ mm) for flint, 10.61 kN ($t = 13.88$ mm) for basalt, and 11.64 kN ($t = 20.00$ mm) for obsidian. The R^2 values increase from flint to basalt to obsidian. This expected increase in R^2 value represents an increase in homogeneity and isotropy. The obsidian is essentially free of visible voids, discontinuities and defects and fracture load increases nearly linearly with thickness. The flint specimens contained several defects and two specimens that varied by 0.14 mm in thickness experienced a 2.24 kN difference in peak load.

An additional measure of comparing the mechanical behavior of the three material types is to examine peak fracture loads for specimens of different material and similar thickness. Table 5 compares the average peak fracture load for specimens of all three materials for two ranges of thickness. Here the percent differences in average peak load for different materials of similar thicknesses range up to −26.88%. Hence, the three distinct equations of linear regression between peak load and thickness, along with the differences in peak load values for similar specimens, indicate that these raw materials were indeed mechanically distinct.

2.3. Main analyses

2.3.1. Handaxe shape assessment

For every handaxe replica and the target model, a set of 29 morphometric variables was obtained (Fig. 12). Measurements were obtained digitally by importing photographic images of each replica into Adobe Illustrator. Images were obtained with a Fujifilm DSLR camera securely attached to a copystand (30× zoom lens: 24–720 mm). A standardized orientation protocol was applied in order to obtain homologous measurements. The orientation protocol applied has previously been described by Schillinger et al. (2014), which is a modified version of that originally designed by Callow (1976). To implement the orientation protocol, the maximum length line for each handaxe was identified in plan-view. The terminus of this line at the more pointed end of the handaxe defined the "tip." Thereafter, each handaxe model was orientated through the tip such that the two longest orthogonal lines diverging from a second length line (i.e. "length by orientation") were both equal in length (see Schillinger et al., 2014:Fig. 3).

To obtain the dataset, a digital grid was placed onto each handaxe image in both plan-view and profile-view (Fig. 12). The measurement grid was superimposed onto digital images of each handaxe so that the grid's central line was positioned directly on the maximum length line (defined by orientation). Thereafter, the upper and lower boundaries of the grid were adjusted to the maximum length dimensions of each handaxe. Horizontal lines were positioned at equally-spaced distances (10% increments) along the length. Additional gridlines were placed at 5%, 15%, 85%, and 95% of length. These additional measurements were taken in order to capture particular variation in shape around the "tip" and "base" of each handaxe. Profile-views were obtained by turning the orientated replica through an axis of 90° such that all thickness measurements were taken orthogonal to the plan-view measurements. Grid boundaries were then repositioned on the maximum length of each handaxe (Fig. 12). Maximum width and maximum thickness were also taken for each handaxe (Fig. 12). Measurements were subsequently obtained digitally using Adobe Illustrator.

In order to transform the dimensional data obtained into shape variables, all morphometric data were size-adjusted using the geometric mean method (Jungers et al., 1995; Lycett et al., 2006). This method of size-adjustment effectively removes scaling (i.e. size) variation between specimens by equalizing their volumes, yet retains their relevant shape data (Falsetti et al., 1993; Jungers et al., 1995). The geometric mean of a series of n variables ($a_1, a_2, a_3 \ldots a_n$) is equivalent to $(a_1 \times a_2 \times a_3 \times \ldots \times a_n)^{1/n}$. Simply, the geometric mean is the nth root of the product of all n variables (Sokal and Rohlf, 1995). The method proceeds on a specimen-by-specimen basis, dividing each variable in turn by the geometric mean of the variables to be size-adjusted. Hence, to implement the method, the geometric mean of each handaxe was computed separately and, thereafter, each of the 29 morphometric variables were divided by that particular handaxe's geometric mean. This was repeated for all handaxes used in the analyses.

2.3.2. Handaxe shape assessment: predictions

If, as predicted by the raw material constraints hypothesis, stone raw material differences determine handaxe form, then: (1) there should be statistically significant inter-group shape differences between two or more raw material groups; and (2), one or more raw material groups should deviate significantly in shape from the model more so than other categories.

We tested the first prediction via a MANOVA of the 29 handaxe shape variables, where $\alpha = 0.05$ using two different test statistics (Pillai's Trace and Wilks' Lambda). In addition, we undertook a Principal Components Analysis (PCA) including the model handaxe in order to visualize major shape variation among the three raw material categories relative to the target model handaxe.

We formally tested the second prediction by computing multivariate Euclidean distances between each replica handaxe and the model using all resultant PC scores (i.e. 100% of variance explained). We tested for significant differences in average shape divergence between replicas and the model across the three raw material categories using a one-way ANOVA.

2.3.3. Production economy

Production economy, i.e. the efficiency by which original starting mass is reduced within the context of defined knapping goals,

Table 3
Linear regression of peak load vs. specimen thickness.

	Eq.	Linear regression	R^2	P
Basalt	1	$y = 0.913x - 4.74$	0.828	<0.0001
Flint	2	$y = 1.45x - 9.75$	0.771	<0.0001
Obsidian	3	$y = 0.734x - 2.79$	0.947	<0.0001

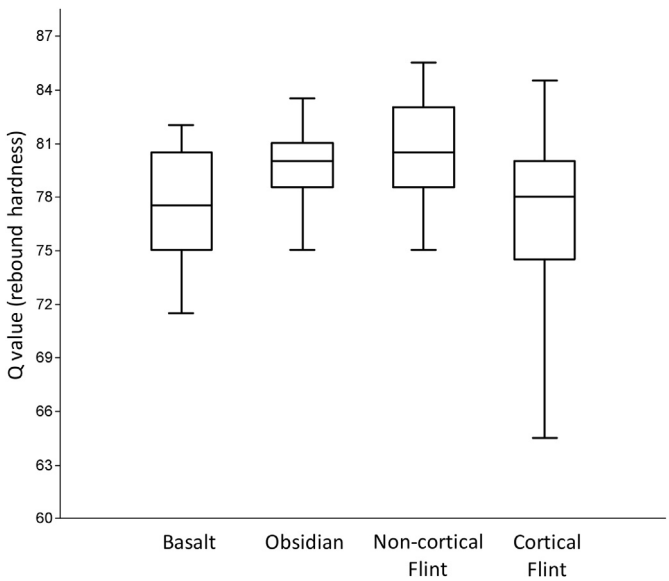

Fig. 8. Boxplots of rebound hardness values across different raw material surfaces (box ranges indicate 25–75% quartiles, with median values shown as bar within).

may have been a specific motivating factor in the use of certain reduction strategies by hominins across time and space (Brantingham and Kuhn, 2001; Brantingham, 2010; Lycett and Eren, 2013). Economic factors may be particularly relevant when the knapping goal is to produce an artifact of specific shape (Eren et al., 2011b), since because knapping is an inherently "reductive" process, the only correction strategy available to a knapper when errors of shape occur is to remove more material (i.e. mass) (Schillinger et al., 2014). Hence, in addition to analyzing handaxe shape, we also measured handaxe production economy. In the event that no differences in handaxe shape were found (i.e. raw material differences did not affect handaxe shape) this

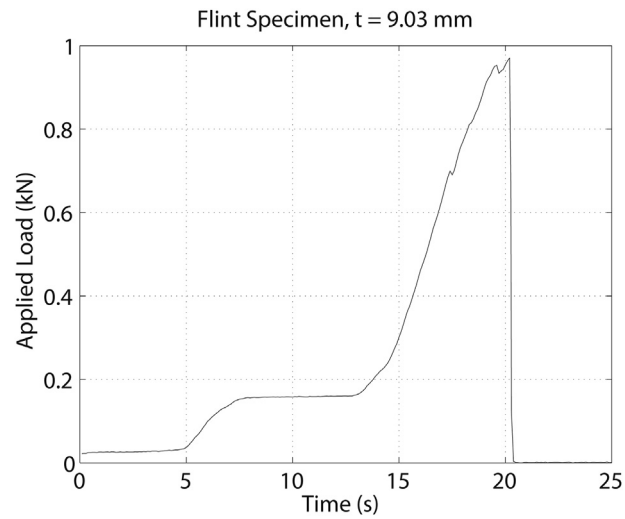

Fig. 10. Example of applied load lime history for flint specimen.

measurement was recorded to assess whether there were differences in how much raw material was used to achieve final handaxe shape. Production economy was computed by dividing the mass of a finished handaxe by the mass of the original nodule from which it was knapped.

2.3.4. Production economy: predictions

If raw material type is affecting production economy systematically (i.e. the amount of nodule mass consumed in producing the handaxe copies differs across raw materials), we would expect statistically significant differences for economy measures between groups. Hence, the null hypothesis is that there would be no statistical differences in the production economy values computed for different categories of raw material. This hypothesis was tested using a Kruskal–Wallis test, where $\alpha = 0.05$. In addition, Levene's test for homogeneity of variances was also applied ($\alpha = 0.05$).

3. Results

3.1. Handaxe shape assessment

Figs. 13 and 14 show the plan-view and profile-view of each raw material's handaxe specimen with the least, average, and most copy-error is directly compared to the model.

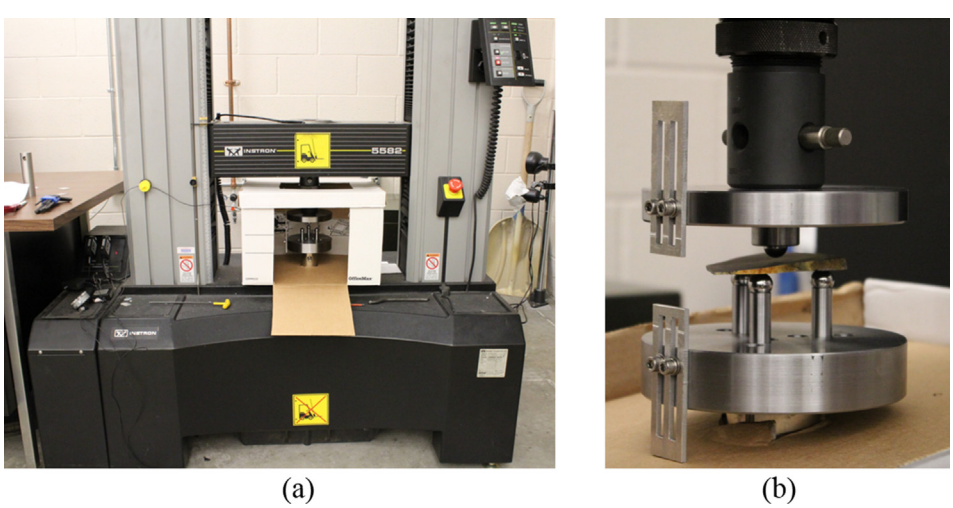

Fig. 9. Experimental setup used for biaxial flexure testing. (a) Axial load frame (b) Biaxial flexure apparatus.

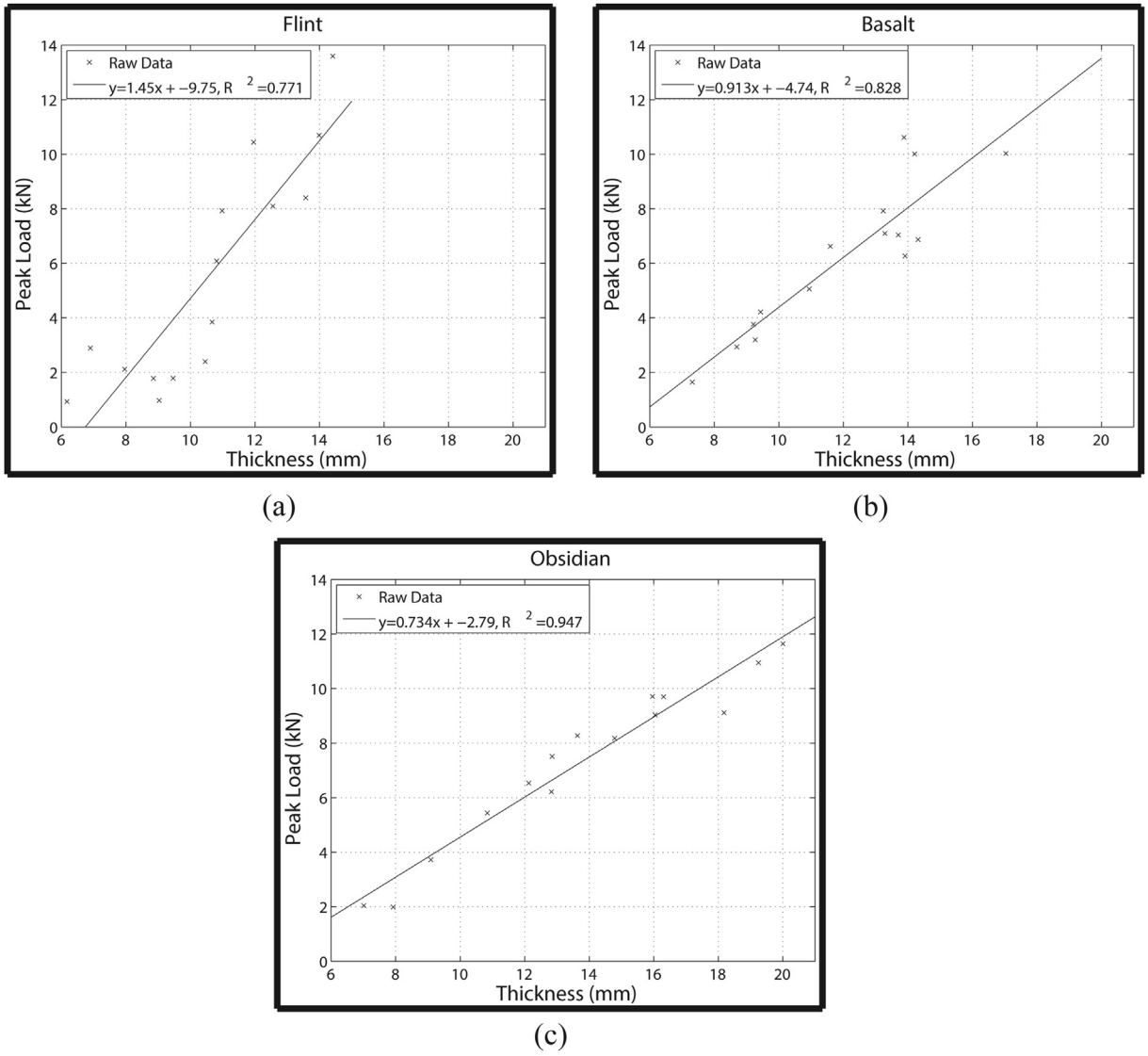

Fig. 11. Peak Load vs. Specimen Thickness (a) Flint (b) Basalt (c) Obsidian.

The MANOVA of all 29 size-adjusted variables showed no significant differences in overall shape across artifact groups made on the three different categories of raw material (Pillai's Trace: $F = 0.902$, df $= 150$, $p = 0.668$; Wilks' Lambda: $F = 0.893$, df $= 148$, $p = 0.684$). Hence, handaxe shape was not significantly different in any of the three raw material categories.

Figs. 15 and 16 show the principal components plots of the first three PC scores (cumulatively accounting for 59.5% of total variance) for all 105 replica handaxes plus the target model. As can be seen, the model falls close to the center of the distribution with raw material categories distributed around the target form.

The ANOVA of the Euclidean distance divergences from the model showed no significant differences across raw material categories ($F = 1.886$; $p = 0.157$). Hence, none of the handaxe groups differed from the model to a greater extent than the other groups.

3.2. Production efficiency assessment

The Kruskal–Wallis test indicated no significant differences between the production economy measures for different raw material types ($H = 2.947$; $p = 0.229$). Hence, production economy was

Table 4
Average peak force for differing specimen thicknesses across materials.

Thickness range	Average peak force (kN)			% Difference (in reference to flint)	
	Flint	Basalt	Obsidian	Basalt	Obsidian
9–11 mm	3.83	4.05	4.58	5.74	19.58
13–15 mm	10.9	7.97	8.23	−26.88	−24.50

Table 5
Mann–Whitney comparisons of hardness (rebound, Q values) values for different raw materials.

	Basalt	Obsidian	Non-cortical flint
Basalt	–	–	–
Obsidian	**0.003**	–	–
Non-cortical flint	**<0.001**	0.314	–
Cortical Flint	0.877	**0.016**	**0.004**

Significant values are shown in bold. Initial Kruskal–Wallis test ($p = 0.0005$).

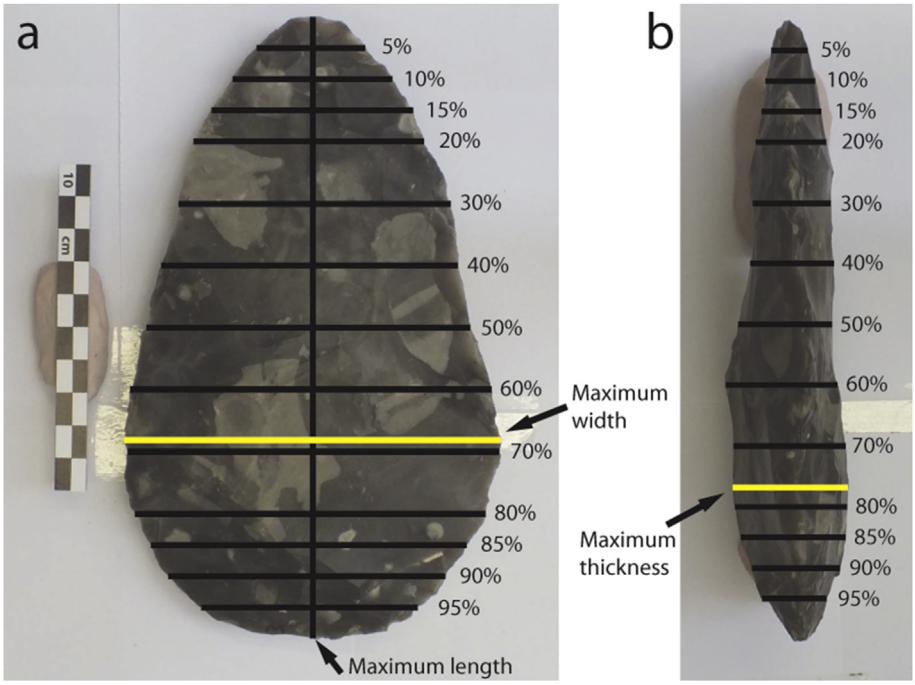

Fig. 12. A digital grid was placed onto each handaxe image in both plan-view (a) and profile-view (b), as illustrated here by the handaxe model, resulting in 29 morphometric variables. The yellow lines indicate maximum width (in a) and maximum thickness (in b). (For interpretation of the references to color in this figure legend, the reader is referred to the web version of this article.)

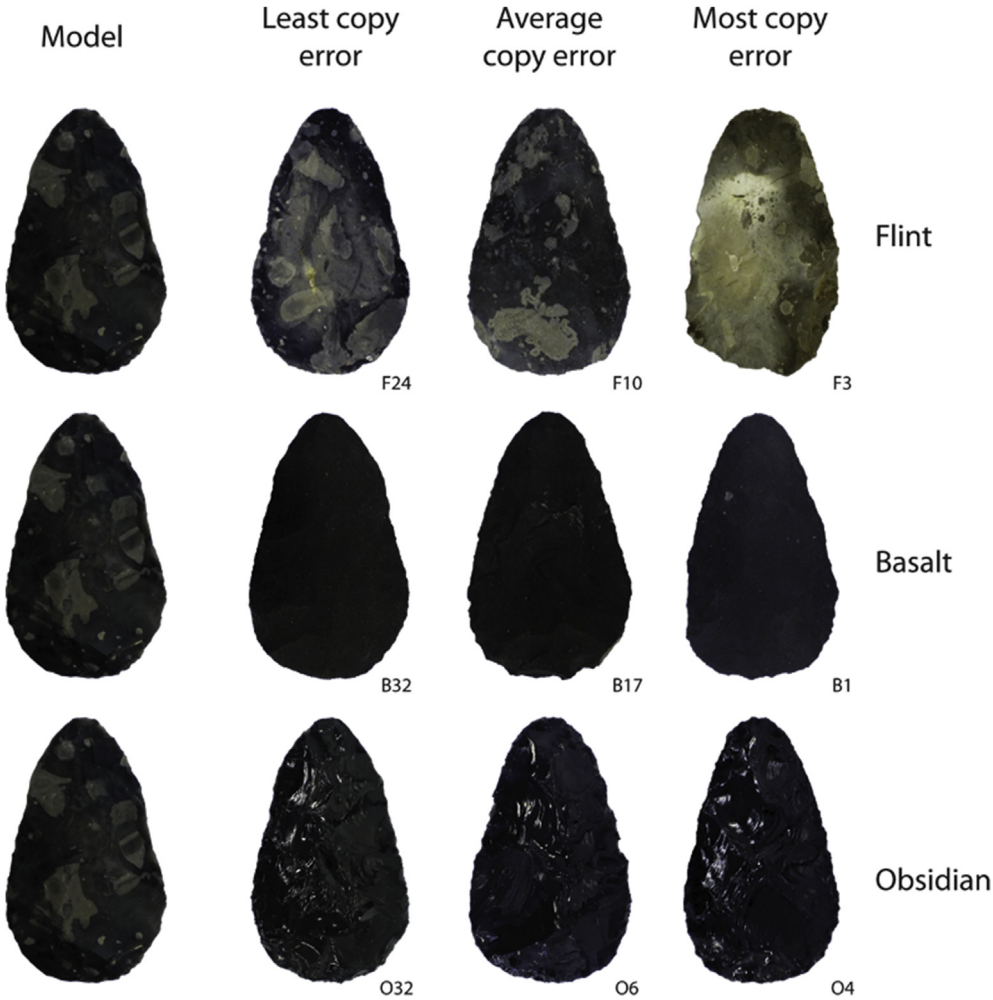

Fig. 13. The model handaxe plan-view (left column) as compared to the handaxe specimen with the least, average, and most copy error from each raw material.

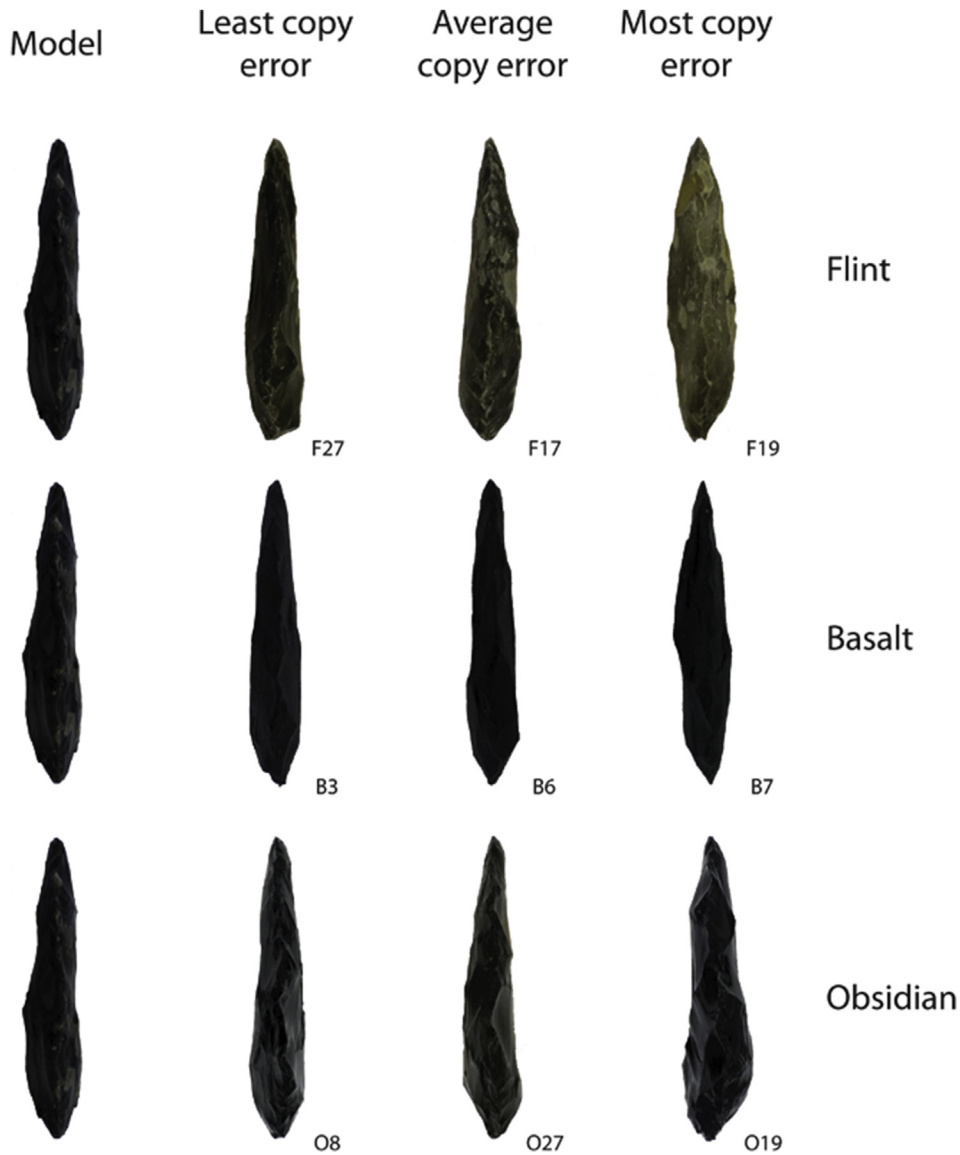

Fig. 14. The model handaxe profile-view (left column) as compared to the handaxe specimen with the least, average, and most copy error from each raw material.

not significantly different across raw materials in terms of central tendencies.

Levene's test for homogeneity of variances did, however, indicate statistical differences ($p = 0.002$). Fig. 17 shows the variation in computed production efficiency values across the three different raw material categories in the form of box plots. As can be seen in Fig. 17, this difference in economy values in terms of variances is driven by values recorded for basalt.

4. Discussion

Understanding the role that raw material plays in the morphology of artifact form has been debated for over a century. We thus designed a replication experiment to assess whether raw material automatically influenced handaxe morphology by testing whether an experienced knapper could copy a model handaxe on three different raw materials: flint, basalt, and obsidian. We demonstrated that these toolstones differed substantially in both their external and internal properties via a series of laboratory tests, empirical observations, and statistical tests. If, as predicted by the raw material constraints hypothesis, stone raw material differences determine handaxe form, then (1) there should be significant intergroup shape differences between two or more raw material groups; and (2), one or more raw material groups should deviate to a significantly greater extent in shape from the model than other groups. We tested these predictions via a series of statistical analyses and a measurement protocol designed to capture the overall shape of each handaxe, consisting of 29 size-adjusted morphometric variables. Our results showed no significant differences in overall shape between the replicated artifacts made on the three raw materials.

No differences in central tendencies between sets of measurements recording production efficiency were detected in our analyses across differing raw materials. However, we did find statistical evidence that use of certain raw materials (in this case basalt) may lead to greater variability of production economy. Raw material factors may, therefore, contribute to the variability of reduction economies seen in archaeological assemblages, but as our analyses also show, these need not significantly affect measures of central tendency. These economy results are particularly interesting given

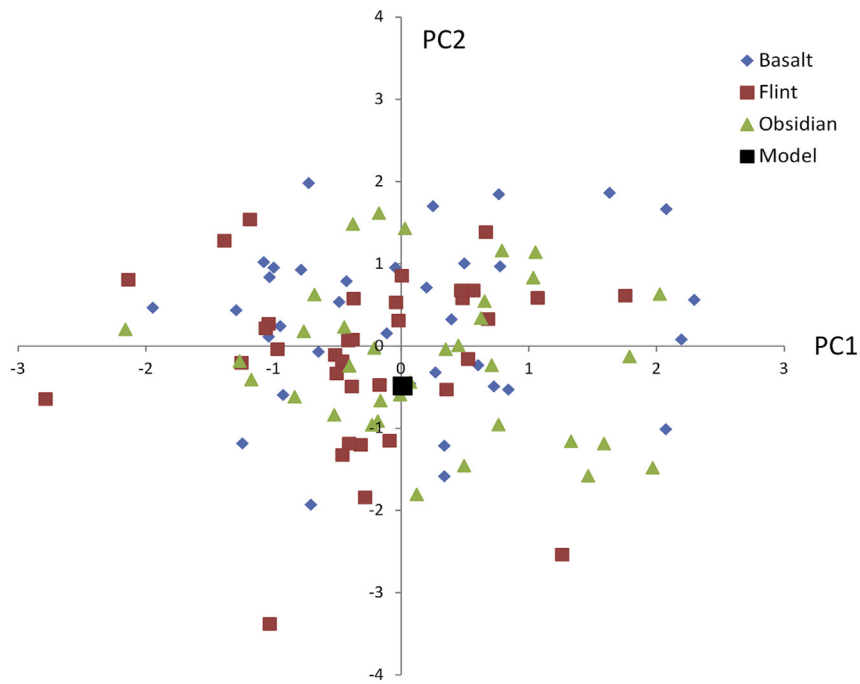

Fig. 15. Plot of PCA results (29 size adjusted variables). PC1 = 36.4% and PC2 = 12.1% of total variance explained. Note position of model close to center of distribution.

that the initial sizes *and* shapes of the nodules were significantly different across raw material categories. As Schillinger et al. (2014) noted recently, when a knapper attempts to copy the shape of another artifact and errors arise during this process, the only strategy by which a knapper can correct that error is to remove more material (i.e. more mass). Our results indicate that differences in raw material categories were not significantly influencing such errors here in any systematic manner.

It should be emphasized that these results do *not* imply that raw materials play no role in within- and between-assemblage patterns of morphological variation in stone tools. What they do, however, emphasize is the inherent danger of assuming that just because morphometric variables differ between sites *and* raw materials at those sites differ, such differences can be glibly attributed to raw material factors. Causation for raw material factors needs to be determined on a case-by-case basis, and must be made on the basis

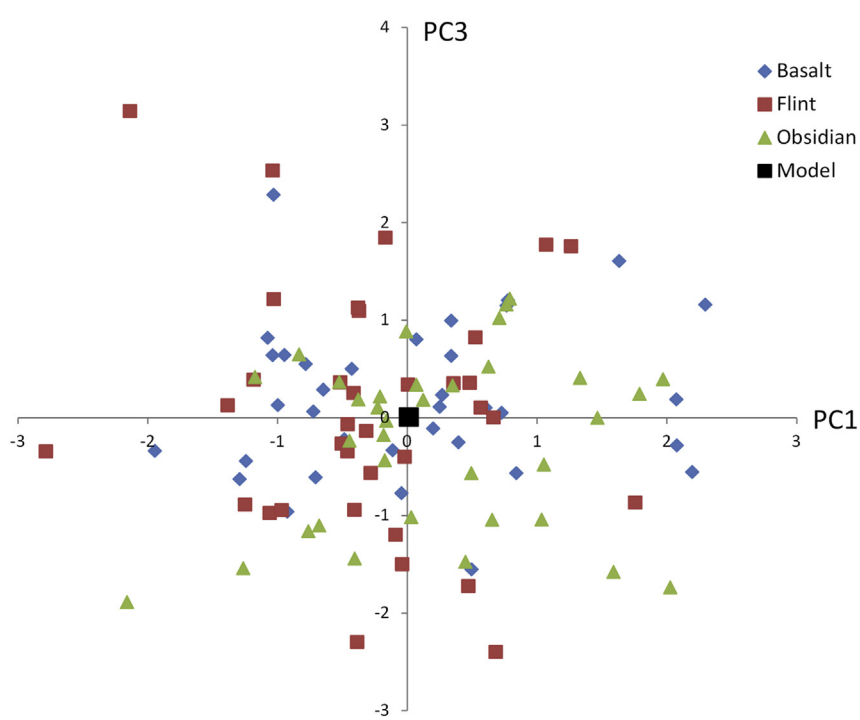

Fig. 16. Plot of PC1 (36.4% of variance explained) and PC3 (11.0% of variance). Note position of model close to center of distribution.

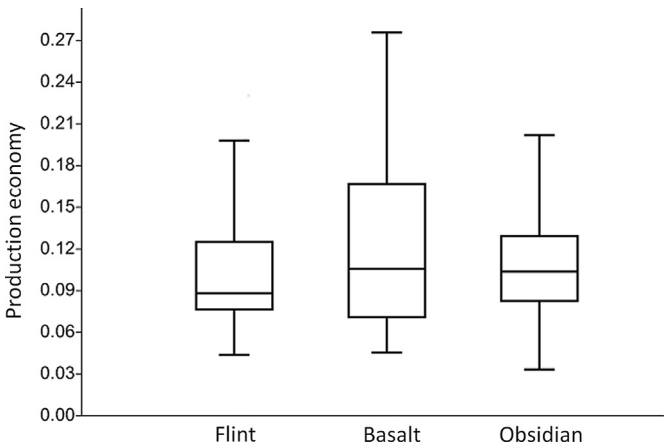

Fig. 17. Box plots of production economy values across different raw materials (box ranges indicate 25–75% quartiles with median values shown as bar within). It is important to note that these production economy values are relevant only within the context and explicitly stated goals of the present experiment.

of formal analysis not merely on the basis of casual observation or association.

One reason to be particularly cautious of informal assertions that raw material factors are determining tool morphology is that rocks used to make stone tools are not necessarily a random sample, an observation Lubbock (1865:33) made nearly 150 years ago. Recent studies have shown that living nonhuman apes can attend to tool properties such as mass and rigidity (Manrique et al., 2010; Schrauf et al., 2012). On the grounds of phylogenetic parsimony, there is no reason to assume that attendance to physical properties of rocks used for knapping was not used as selection criteria for toolstones. Indeed, there is evidence that from at least Oldowan times, hominins were selecting raw materials in a manner that differs proportionally from their local availability (Stout et al., 2005; Harmand, 2009). Moreover, there is evidence that Oldowan hominins were selecting rock types based on the durability of flakes that could be produced (Braun et al., 2009). Given these considerations, it must be remembered that rocks used to make stone tools will in most cases fit within a discrete band of variation in terms of their physical properties, thus in turn restricting the potential influence that raw material properties have in determining within- and between-assemblage patterns of variation. Given these factors, there are no sound reasons to assume that raw material factors will automatically comprise the dominant source of within- and between-assemblage patterns of artifactual variation.

There has sometimes been the assumption that stone is not a particularly "plastic" material, and so is potentially limited in its capacity to reflect behavioral factors (e.g., Gero, 1989: 103–104). The reductive character of stone tool production certainly creates particular internal dynamics that will potentially affect patterns of variation (Baumler, 1995; Schillinger et al., 2014). Indeed, there is evidence that an interplay between the particular reduction strategies adopted by hominins and raw material factors may have taken place in certain times and places, evincing a not invariant relationship between behavioral and natural, lithological factors (Brantingham et al., 2000; Brantingham, 2003, 2010; Gurtov and Eren, 2014). However, our results suggest that the potential for behavior to countermand differences between the external and internal properties of different raw material categories *within* the general media of stone tool production is potentially a potent one.

It must again, however, be noted that we are *not* suggesting that raw material plays no role in shaping stone tool attributes. Indeed, two factors stand out as noteworthy points in respect to the specifics of our experimental results. Firstly, other technologies––for example, the production of Solutrean laurel leaf points or stone "daggers" during the Scandinavian Late Neolithic––may be more subservient to stone tool constraints than our results alone imply, the specialized character of such artifacts notwithstanding (Apel, 2008; Aubry et al., 2008). Secondly, particular raw materials not considered here––such as quartz or sandstone for instance––may have more potent effects than indicated by the analyses we report. These caveats aside, however, our results caution against injudicious assumptions that merely because stone media at two or more sites differ, and metric attributes of artifacts found at those same sites differ, causation for the latter must reside in the former. Indeed, our results are in accordance with a range of archaeological studies implying that factors other than raw materials must rigorously be sought to fully explain differences in the attributes of classes of stone artifacts found across time and space (e.g., Sharon, 2008; Clarkson, 2010; Costa, 2010; Smallwood, 2012; Buchanan et al., 2014; Lycett and von Cramon-Taubadel, 2014).

One cautionary implication must also, however, be emphasized in the light of our results. As noted at the outset, as an alternative to a pure "constraints" hypothesis, raw material factors may have influenced stone artifact morphology because hominins did not possess the knowledge, manual dexterity, skills, or incentive to tackle "challenging" raw materials. As noted, this hypothesis does not suggest that raw material plays no role in artifact form, but instead that it cannot be assumed automatically that there are inherent lithological properties that definitively influence artifact morphology in particular ways. In light of these considerations, what our results perhaps indicate is that rather than presuming *a priori* that raw material is a dominant factor, a key issue is to try and determine how raw material effects are interacting with other relevant factors (Diez-Martin and Eren, 2012:338; Stout, 2005). Indeed, these results perhaps highlight that lithic analytical methods must be further refined—both conceptually and in practical terms—to take account of the simultaneous role that factors such as "skill," "culture," "raw material," and/or "reduction" may be playing in generating within- and between-assemblage patterns of variation (Archer and Braun, 2010; Lycett and von Cramon-Taubadel, 2014). Certainly, an assumed preeminence for raw material "constraints" cannot be justified in light of our results.

Acknowledgments

We are grateful to Craig Ratzat of Neolithics and Alastair Key for their assistance in sourcing the raw material used in our analyses. Kerstin Schillinger provided technical assistance, for which we are indebted. The undertaking of this research was possible thanks to the Leverhulme Trust, which awarded MIE an Early Career Fellowship (ECF-2011-567), and provided additional funding for all materials and procedures. MIE is grateful to Rebecca Catto, and Mustafa, Kathleen, and Nimet Eren for their support.

References

Abbott, W.J.L., 1911. On the classification of the British Stone Age industries and some new, and little known, well-marked horizons and cultures. J. R. Anthropol. Inst. 41, 458–480.
Andrefsky Jr., W., 1994. Raw-Material availability and the organization of technology. Am. Antiq. 59, 21–34.
Andrefsky, W., 1998. Lithics: Macroscopic Approaches to Analysis. Cambridge University Press, Cambridge.
Apel, J., 2008. Knowledge, know-how, and raw material – the production of Late Neolithic flint daggers in Scandinavia. J. Archaeol. Method Theory 15, 91–111.
Archer, W., Braun, D.R., 2010. Variability in bifacial technology at Elandsfontein, Western cape, South Africa: a geometric morphometric approach. J. Archaeol. Sci. 37, 201–209.

Ashton, N., McNabb, J., 1994. Bifaces in perspective. In: Ashton, N., David, A. (Eds.), Stories in Stone: Lithic Studies Society Occasional Paper No.4. Lithic Studies Society, London, pp. 182–191.
Aubry, T., Bradley, B., Almeida, M., Walter, B., Neves, M., Pelegrin, J., Lenoir, M., Tiffagom, M., 2008. Solutrean laurel leaf production at Maîtreaux: an experimental approach guided by techno-economic analysis. World Archaeol. 40, 48–66.
Bar-Yosef, O., Eren, M.I., Yuan, J., Cohen, D., Li, Y., 2012. Were bamboo tools made in prehistoric Southeast Asia? An experimental view from South China. Quat. Int. 269, 9–21.
Baumler, M.F., 1995. Principles and properties of lithic core reduction: implications for Levallois technology. In: Dibble, H.L., Bar-Yosef, O. (Eds.), The Definition and Interpretation of Levallois Technology. Prehistory Press, Madison, Wisconsin, pp. 11–23.
Beck, M., 2002. The ball-on-three-ball test for tensile strength: refined methodology and results for three Hohkam ceramic types. Am. Antiq. 67, 558–569.
Brantingham, P.J., 2003. A neutral model of stone raw material procurement. Am. Antiq. 68, 487–509.
Brantingham, P.J., 2010. The mathematics of *chaîne opératoires*. In: Lycett, S.J., Chauhan, P.R. (Eds.), New Perspectives on Old Stones: Analytical Approaches to Paleolithic Technologies. Springer, New York, pp. 183–206.
Brantingham, P.J., Kuhn, S.L., 2001. Constraints on Levallois core technology: a mathematical model. J. Archaeol. Sci. 28, 747–761.
Brantingham, P.J., Olsen, J.W., Rech, J.A., Krivoshapkin, A.I., 2000. Raw material quality and prepared core technologies in Northeast Asia. J. Archaeol. Sci. 27, 255–271.
Braun, D.R., Plummer, T., Ferraro, J.V., Ditchfield, P., Bishop, L.C., 2009. Raw material quality and Oldowan hominin toolstone preferences: evidence from Kanjera South, Kenya. J. Archaeol. Sci. 36, 1605–1614.
Browne, C., Wilson, L., 2011. Resource selection of lithic raw materials in the Middle Palaeolithic in southern France. J. Hum. Evol. 61, 597–608.
Buchanan, B., O'Brien, M., Collard, M., 2014. Continent-wide or region-specific? A geometric morphometrics-based assessment of variation in Clovis point shape. Archaeol. Anthropol. Sci. 6, 145–162.
Callahan, E., 1979. The basics of biface knapping in the eastern fluted point tradition: a manual for flintknappers. Archaeol. East. N. Am. 7, 1–180.
Callow, P., 1976. The Lower and Middle Palaeolithic of Britain and Adjacent Areas of Europe (PhD thesis). University of Cambridge, Cambridge.
Clark, J.D., 2001. Variability in primary and secondary technologies of the later Acheulian in Africa. In: Milliken, S., Cook, J. (Eds.), A Very Remote Period Indeed: Papers on the Palaeolithic Presented to Derek Roe. Oxbow Books, Oxford, pp. 1–18.
Clarkson, C., 2010. Regional diversity within the core technology of the Howiesons Poort techno-complex. In: Lycett, S.J., Chauhan, P.R. (Eds.), New Perspectives on Old Stones: Analytical Approaches to Paleolithic Technologies. Springer, New York, pp. 43–59.
Costa, A.G., 2010. A geometric morphometric assessment of plan shape in bone and stone Acheulean bifaces from the Middle Pleistocene site of Castel di Guido, Latium, Italy. In: Lycett, S.J., Chauhan, P.R. (Eds.), New Perspectives on Old Stones: Analytical Approaches to Paleolithic Technologies. Springer, New York, pp. 23–41.
Crabtree, D.E., 1967. Notes on experiments in flintknapping: 3. The flintknappers raw materials. Tebiwa 10, 8–25.
de la Torre, I., 2011. The Early Stone Age lithic assemblages of Gadeb (Ethiopia) and the Developed Oldowan/early Acheulean in East Africa. J. Hum. Evol. 60, 768–812.
Diez-Martin, F., Eren, M.I., 2012. The Early Acheulean in Africa: past paradigms, current ideas, and future directions. In: Dominguez-Rodrigo, M. (Ed.), Stone Tools and Fossil Bones: Debates in the Archaeology of Human Origins. Cambridge University Press, Cambridge, pp. 310–358.
Domanski, M., Webb, J., Boland, J., 1994. Mechanical properties of stone aretfact materials and the effect of heat treatment. Archeometry 36, 177–208.
Edwards, S.W., 2001. A modern knapper's assessment of the technical skills of the Late Acheulean biface workers at Kalambo Falls. In: Clark, J.D. (Ed.), Kalambo Falls Prehistoric Site, vol. III. Cambridge University Press, Cambridge, pp. 605–611.
Eren, M.I., Lycett, S.J., Roos, C.I., Sampson, C.G., 2011a. Toolstone constraints on knapping skill: Levallois reduction with two different raw materials. J. Archaeol. Sci. 38, 2731–2739.
Eren, M.I., Bradley, B.A., Sampson, C.G., 2011b. Middle Paleolithic skill-level and the individual knapper: an experiment. Am. Antiq. 76, 229–251.
Falsetti, A.B., Jungers, W.L., Cole III, T.M., 1993. Morphometrics of the Callitrichid forelimb: a case study in size and shape. Int. J. Primatol. 14, 551–572.
Gero, J.M., 1989. Assessing social information in material objects: how well do lithics measure up? In: Torrence, R. (Ed.), Time, Energy and Stone Tools. Cambridge University Press, Cambridge, pp. 92–105.
Goodman, M.E., 1944. The physical properties of stone tool materials. Am. Antiq. 9, 415–433.
Goodyear, A., 1989. A hypothesis for the use of cryptocrystalline raw materials among Paleoindian groups of North America. In: Ellis, C., Lothrop, J. (Eds.), Eastern Paleoindian Lithic Resource Use. Westview Press, Boulder, pp. 1–10.
Gowlett, J.A.J., 2011. The Empire of the Acheulean strikes back. In: Sept, J., Pilbeam, D. (Eds.), Casting the Net Wide: Papers in Honor of Glynn Isaac and His Approach to Human Origins Research. American School of Prehistoric Research, Cambridge, MA, pp. 93–114.
Gurtov, A.N., Eren, M.I., 2014. Lower Paleolithic bipolar reduction and hominin selection of quartz at Olduvai Gorge, Tanzania: what's the connection? Quat. Int. 322–323, 285–291.
Harmand, S., 2009. Variability in Raw Material Selectivity at the Late Pliocene sites of Lokalalei, West Turkana, Kenya. In: Hovers, E., Braun, D.R. (Eds.), Interdisciplinary Approaches to the Oldowan. Springer, Dordrecht, pp. 85–97.
Holdoway, S., Stern, N., 2004. A Record in Stone: the Study of Australia's Flaked Stone Artefacts. Victoria Museum, Melbourne.
Isaac, G.L., 1977. Olorgesailie: Archaeological Studies of a Middle Pleistocene Lake Basin in Kenya. University of Chicago Press, Chicago.
Jennings, T.A., Pevny, C.D., Dickens, W.A., 2010. A biface and blade core efficiency experiment: implications for Early Paleoindian technological organisation. J. Archaeol. Sci. 37, 2155–2164.
Jones, P.R., 1979. Effects of raw material on biface manufacture. Science 204, 835–836.
Jungers, W.L., Falsetti, A.B., Wall, C.E., 1995. Shape, relative size, and size adjustments in morphometrics. Yearb. Phys. Anthropol. 38, 137–161.
Lubbock, J., 1865. Prehistoric Times. Williams and Norgate, London.
Luedtke, B.E., 1992. An Archaeologist's Guide to Chert and Flint. Institute of Archaeology, University of California, Los Angeles.
Lycett, S.J., Bae, C.J., 2010. The Movius Line controversy: the state of the debate. World Archaeol. 42, 521–544.
Lycett, S.J., Eren, M.I., 2013. Levallois economics: an examination of 'waste' production in experimentally produced Levallois reduction sequences. J. Archaeol. Sci. 40, 2384–2392.
Lycett, S.J., von Cramon-Taubadel, N., 2014. Toward a "quantitative genetic" approach to lithic variation. J. Archaeol. Method Theory. http://dx.doi.org/10.1007/s10816-013-9200-9.
Lycett, S.J., von Cramon-Taubdel, N., Foley, R., 2006. A crossbeam co-ordinate caliper for the morphometric analysis of lithic nuclei: a description, test, and empirical examples of application. J. Archaeol. Sci. 33, 847–861.
Manrique, H.M., Nam-mi Gross, A., Call, J., 2010. Great apes select tools on the basis of their rigidity. J. Exp. Psychol. Anim. Behav. Process. 36, 409–422.
McPherron, S., 2006. Variability in Acheulian handaxe morphology and its implications for typology. In: Goren-Inbar, N., Sharon, G. (Eds.), Axe Age: Acheulian Toolmaking: From Quarry to Discard (Approaches to Anthropological Archaeology). Equinox Publishing, London, pp. 267–285.
Manninen, M., Knutsson, K., 2014. Lithic raw material diversification as an adaptive strategy – technology, mobility, and site structure in Late Mesolithic northernmost Europe. J. Anthropol. Archaeol. 33, 84–98.
Neupert, M.A., 1994. Strength testing archaeological ceramics: a new perspective. Am. Antiq. 59, 709–723.
Ritter, J.E., Jakus, K., Batakis, A., Bandyopadhyay, N., 1980. Appraisal of biaxial strength testing. J. Non-cryst. Solids 38–39, 419–424.
Roe, D.A., 1994. A metrical analysis of selected sets of handaxes and cleavers from Olduvai Gorge. In: Leakey, M.D., Roe, D.A. (Eds.), Olduvai Gorge, vol. 5. Cambridge University Press, Cambridge, pp. 146–234.
Schick, K.D., 1994. The Movius line reconsidered. In: Corruccini, R.S., Ciochon, R.L. (Eds.), Integrative Paths to the Past. Prentice Hall, Englewood Cliffs, NJ, pp. 569–596.
Schillinger, K., Mesoudi, A., Lycett, S.J., 2014. Copying error and the cultural evolution of "additive" vs. "reductive" material traditions: an experimental assessment. Am. Antiq. 79, 128–143.
Schrauf, C., Call, J., Fuwa, K., Hirata, S., 2012. Do chimpanzees use weight to select hammer tools? PLoS One 7, e41044.
Sharon, G., 2008. The impact of raw material on Acheulian large flake production. J. Archaeol. Sci., 1329–1344.
Smallwood, A., 2010. Clovis biface technology at the Topper site, South Carolina: evidence for variation and technological flexibility. J. Archaeol. Sci. 37, 2413–2425.
Smallwood, A., 2012. Clovis technology and settlement in the American Southeast: using biface analysis to evaluate dispersal models. Am. Antiq. 77, 689–713.
Sokal, R.R., Rohlf, F.J., 1995. Biometry. W.H. Freeman & Co, New York.
Stout, D., 2005. The social and cultural context of stone-knapping skill acquisition. In: Roux, V., Bril, B. (Eds.), Stone Knapping: the Necessary Conditions for a Uniquely Hominin Behavior. McDonald Institute for Archaeological Research, Oxford, pp. 331–340.
Stout, D., Quade, J., Semaw, S., Rogers, M., Levin, N., 2005. Raw material selectivity of the earliest stone toolmakers at Gona, Afar, Ethiopia. J. Hum. Evol. 48, 365–380.
Whittaker, J.C., 1994. Flintknapping: Making and Understanding Stone Tools. University of Texas Press, Austin.
Winton, V., 2005. An investigation of knapping-skill development in the manufacture of Palaeolithic handaxes. In: Roux, V., Bril, B. (Eds.), Stone Knapping: the Necessary Conditions for a Uniquely Hominin Behavior. McDonald Institute for Archaeological Research, Oxford, pp. 109–116.
Wynn, T., Tierson, F., 1990. Regional comparison of the shapes of later Acheulean handaxes. Am. Anthropol. 92, 73–84.